

# Railway track switch simulation: a new dynamic model for studying actuator and switch blade dynamics

Proc IMechE Part F:  
J Rail and Rapid Transit  
2022, Vol. 0(0) 1–9  
© IMechE 2022



Article reuse guidelines:  
[sagepub.com/journals-permissions](https://sagepub.com/journals-permissions)  
DOI: 10.1177/09544097221141741  
[journals.sagepub.com/home/pif](https://journals.sagepub.com/home/pif)



Linxiao Li<sup>1</sup> , Saikat Dutta<sup>2</sup> , Roger Dixon<sup>1</sup> and Edward Stewart<sup>1</sup>

## Abstract

This paper proposes a new approach to the dynamic modelling of railway track switches. The approach results in a model which faithfully reproduces the dynamic bending of the switch blades, allows simulated actuators (forces) to be applied along the length of the rails and can be simulated in times that are an order of magnitude faster than similar models in multi-body dynamics software (such as Simpack). These are the main contributions that should be of use to researchers and engineers concerned with the design of switches and their actuation mechanisms. First, an actuator model is developed; then the switch blade FEA (Finite Element Analysis) model is developed and validated against static bending predictions; the two are then combined and validated against the dynamic and steady-state predictions from a validated Simpack model. The complete model can be found here: <https://doi.org/10.25500/edata.bham.00000884>.

## Keywords

Railway track switch, switch blade, finite element analysis, actuator, Simulink, model validation

Date received: 28 April 2022; accepted: 25 October 2022

## Introduction

Track switches are electric or hydraulic mechanical systems installed on the track, which allow railway vehicles to switch from one route to another, thereby providing flexibility for the railway network.<sup>1</sup> There are types of various railway switches in operation in the UK. The most common of these are Clamplock, HPSS, HW, and mechanical point machines.<sup>2,3</sup> Figure 1 gives an equivalent track switch model.

At present, there are a large number of mechanical modelling and design software for structural optimization or dynamic evaluation, such as Simpack in Germany, NUCARS of the North American Railway Association, MSD.ADAMS/Rail, and general mechanical modelling software, such as Abaqus, ANSYS, etc.<sup>4</sup> In the structural design and bending analysis of the switch, the finite element analysis method is widely used. To study the interaction between train and track, Andersson and Dahlberg modelled the turnout through linear finite elements with modal damping.<sup>5,6</sup> Bruni et al. built a detailed three-dimensional finite element model in ABAQUS to study the vehicle's dynamic behaviour when running over turnouts.<sup>7</sup>

Recently, researchers have shown increasing interest in improving the performance, safety, and reliability of the railway network from projects such as S-CODE,<sup>8</sup> In2Rail,<sup>9</sup> and REPOINT.<sup>1</sup> A Reprint switch prototype simulation model is established using McCauley's method in MATLAB/Simulink.<sup>10</sup> The researchers also developed a track switch model using the multi-body simulator Simpack, bending the switch track to a single actuator of a REPOINT-

light switch,<sup>11</sup> and then a full-scale demonstrator for the novel railway track switch was built.<sup>12</sup> Besides, to research and design a new approach to railway track switch actuation, Dutta et al. first modelled a rail unit by finite element analysis (FEA) in ABAQUS, then generated a complete switch system through Simpack, and finally linked it into Simulink to form a co-simulation space.<sup>13</sup> However, this kind of simulation in the co-simulation environment requires an extremely long computational time, approximately several hours to simulate one second. Therefore, it is helpful to utilize a more effective method for research work within a limited time range.

Compared to past work, the key innovation in this paper comes from applying finite element modelling methods, to represent the switch blades, directly in MATLAB/Simulink. This simplifies the model somewhat, removes the need for co-simulation of the track, actuator and control system and results in a single system model. The first benefit is that this significantly reduces the time required to run the model and obtain overall system simulation results. Secondly, independent actuation forces (from separate actuators) can be applied at different locations along the length of the switch blades model. At the same time, the system-level simulation

<sup>1</sup>School of Engineering, University of Birmingham, Birmingham, UK

<sup>2</sup>School of Mechanical Engineering, Coventry University, Coventry, UK

## Corresponding author:

Linxiao Li, Centre for Railway Research and Education, University of Birmingham, Pritchatts Road, Edgbaston, Birmingham B15 2TT, UK.  
Email: [railCM@contacts.bham.ac.uk](mailto:railCM@contacts.bham.ac.uk)

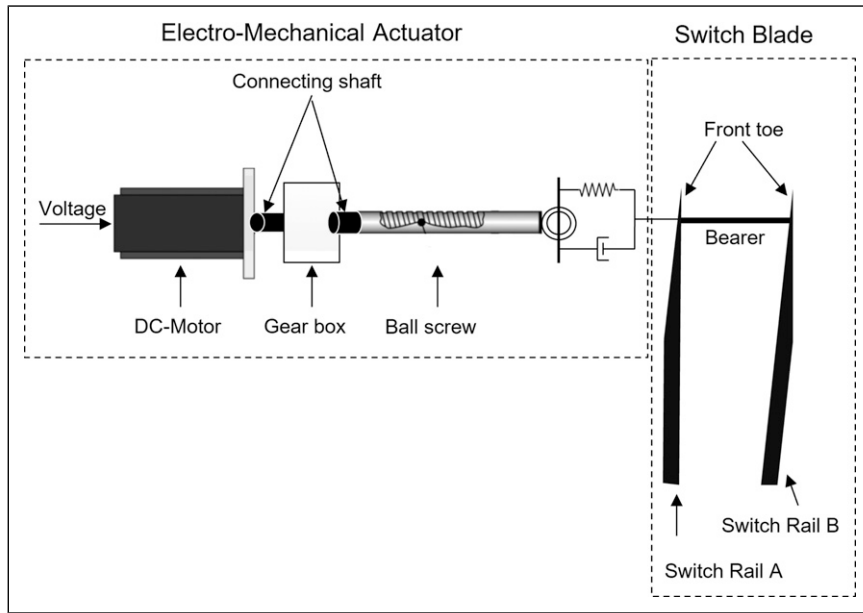


**Figure 1.** Equivalent model of a track switch system.

is able to reproduce the behaviour predicted by the more complex (and significantly slower) co-simulation approach.

The paper is organised as follows. In the (next) modelling section, the actuator model is developed; then, the switch blade static and dynamic FEA model equations are presented. Subsequently, in the simulation results section, the dynamic model is compared with the static bending predictions and the dynamic predictions from a previously published model in Simpack. In the final part of the results section, the actuator and blade (bending) model are combined and validated against the dynamic and steady-state predictions from a validated Simpack model; and a set of static experimental results. The final part of the paper draws conclusions from the work and suggests future directions and uses for the new system-level switch model.

## System modelling

The full switch model is obtained through a physical analysis of its components. The aim is to provide an easily accessible and transparent description of the physical behaviour of the switch. Although different switches in the installation have different parameters, the models and interactions of the sub-components remain the same. In this paper, the switch layout is based on a typical CVS-type switch,<sup>3</sup> and actuation and locking are provided by a High Performance Switch System (HPSS) type machine, with a non-back-drive-able lead screw. The complete switch system is mainly composed of two parts, namely the actuator and the switch blade. The actuator receives power from the line-side cabinet and drives the front toe to move the switch blade from one position to another. Figure 1 gives the structure of the entire track switch system with five main components: the motor model, the gearbox model, the mechanical linkage model, the ball screw model, and the switch blade model. Each of these components is discussed below where a simulation model is shown in Figure 2.

### Electro-Mechanical actuator model

The electro-mechanical actuator model consists of a DC (direct current) motor model, a gearbox model, a mechanical linkage model, and a ball screw model. The motor is connected to the gearbox to achieve speed-reduction. The ball screw converts rotary motion into linear motion. The front toe of the switch rail is connected to the ball screw through mechanical linkages. The parameters of the DC motor, the gearbox, and the ball screw are listed in Table 1.

The motor input voltage,  $V$  drives the motor to cause the motor shaft to rotate at the motor speed of  $\dot{\theta}_m$ . The electrical equations of the DC motor are written by:

$$V = R_m I_m + L_m \dot{I}_m + K_e \dot{\theta}_m \quad (1)$$

$$T_m = K_t I_m \quad (2)$$

where  $R_m$  is the rotor resistance,  $I_m$  is the motor armature current,  $K_e$  is the back EMF (Electro Motive Force) constant of the motor, and  $L_m$  is the rotor inductance. The motor output torque,  $T_m$ , is generated by the angular rotation of the motor shaft.  $K_t$  is the motor torque constant.

The mechanical equation for the motor is derived using Newton's second law of motion, thus, a linear model can be obtained using the torque balancing rule:

$$J_m \ddot{\theta} + D_m \dot{\theta} = T_m - T_{gs} \quad (3)$$

Refer to equation (3)  $T_{gs}$  is the transmitted shaft torque between the motor and the gearbox,  $J_m$  and  $D_m$  represent inertia and damping constant of the motor.

The gearbox is a reduction mechanism that reduces the angular velocity and amplifies the motor's output torque, which is linked with the motor by a connecting shaft.

The transmitted shaft torque equation is described as:

$$T_{gs} = K_s (\theta_m - \theta_{gi}) + C_s (\dot{\theta}_m - \dot{\theta}_{gi}) \quad (4)$$

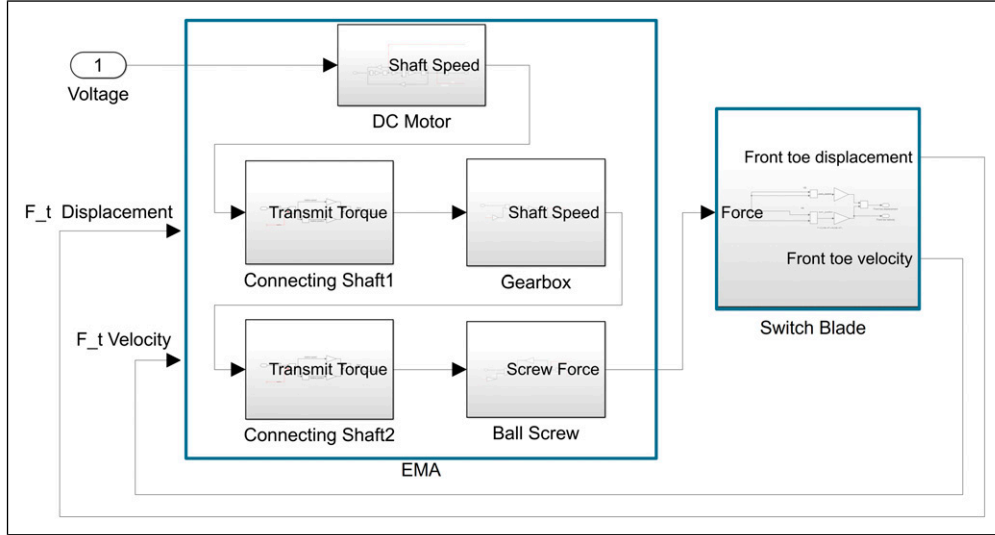


**Figure 2.** Simulation model of the track switch system.

**Table 1.** Parameters of DC motor, gearbox, ball screw and switch blade.

Description	Value	Units
$R_m$ Rotor resistance	2.6	$\Omega$
$L_m$ Area moment of inertia	0.0108	H
$K_e$ Back EMF constant	0.2865	Vrms/(rad/s)
$K_t$ Motor torque constant	0.75	Nm/A
$J_m$ Motor inertia	$7.5 \times 10^{-3}$	kgm <sup>2</sup>
$D_m$ Motor damping constant	$4.01 \times 10^{-4}$	Nm(rad/s)
$J_g$ Gearbox inertial	$2.1 \times 10^{-3}$	kgm <sup>2</sup>
$D_g$ Gearbox damping constant	$3 \times 10^{-4}$	Nm(rad/s)
$n$ Gear ratio	15	—
$J_b$ Ball screw inertial	0.2	kgm <sup>2</sup>
$D_b$ Ball screw damping constant	$0.1 \times 10^{-4}$	Nm(rad/s)
$l$ The lead of the screw	0.008	m
$L$ Length of the switch blade	9.21	m
$I$ Area moment of inertia	$5.6 \times 10^6$	m <sup>4</sup>
$A$ Full area of cross-section	$9.334 \times 10^{-3}$	m <sup>2</sup>
$E$ Young's modulus of steel	$2 \times 10^{11}$	P <sub>a</sub>
$m$ Mass of one switch blade	276.58	kg
$g$ Gravity acceleration	9.81	m/s <sup>2</sup>
$Z_1$ Distance of $P_1$ from free end	2.3	m
$Z_2$ Distance of $P_2$ from free end	0.92	m
$Z_3$ Distance of $P_3$ from free end	0	m

The gearbox mathematical equation is written as:

$$J_g \ddot{\theta} + D_g \dot{\theta} = T_{gs} - \frac{T_{bs}}{n} \quad (5)$$

where  $K_s$  is the shaft stiffness and  $C_s$  the shaft damping.  $\theta_{gi}$  and  $\dot{\theta}_{gi}$  is the gearbox angular position and velocity respectively.  $J_g$  and  $D_g$  is inertia and damping constant of the gearbox,  $n$  is the gear ratio.  $T_{bs}$  is the transmitted shaft torque for the gearbox and ball screw.

The ball screw converts the rotational motion of the connecting shaft into linear motion.  $J_b$  is ball screw inertia,  $D_b$  is the ball screw damping constant. The rotation equations can be written:

$$J_b \ddot{\theta} + D_b \dot{\theta} = T_{bs} - T_l \quad (6)$$

The load torque,  $T_l$  is caused by the reaction force,  $F$ , as the actuator exerts a force on the switch blade. The relationship between the two is described by:

$$T_l = F \frac{l}{2\pi} \quad (7)$$

Assuming that the ball screw and the switch blade are rigidly connected, they can be modelled as a stiff spring-damper assembly. The actuation force can be calculated by the linear motion of the ball screw and the switch blade,

$$F = C_b(v_{lb} - v_{lf}) + K_b(x_{lb} - x_{lf}) \quad (8)$$

where  $C_b$  and  $K_b$  are the damping and stiffness of the ball screw and front toe mechanical assembly. The linear velocities of the ball screw and the front toe are  $v_{lb}$  and  $v_{lf}$ ,  $x_{lb}$  and  $x_{lf}$  are the linear displacements.

The contact force between the switch rail and the stock rail is modelled by an extremely stiff spring and damper which is switching on when the switch blade makes physical contact with the stock rail, the purpose of which is to restrict motion. The contact force  $F_s$  is written by:

$$F_s = \begin{cases} K_r(x_{s1} - x) + C_r(\dot{x}_{s1} - \dot{x})(x < x_{s1}) \\ K_r(x - x_{s2}) + C_r(\dot{x} - \dot{x}_{s2})(x > x_{s2}) \end{cases} \quad (9)$$

where  $x$  is the displacement of the front toe,  $x_{s1}$  and  $x_{s2}$  are the positions of two stock rails,  $K_r$  and  $C_r$  are the damping and stiffness.

### Switch blade model

Two methods are adopted for switch blade modelling in this paper. One is considering the switch blade as a beam to analyse the deflection properties. The second is to use the finite element analysis method to establish a dynamic model in Simulink.<sup>14</sup> The static bending analysis can be regarded as a reference for the dynamic model.

**Static rail model.** When the switch blade is in motion, it is driven by a lateral load. Only one bending mode of the horizontal ( $x$ - $z$  axis) is considered. The bending switch blade is considered as a cantilever beam under the action of the three ideal forces to describe the deflection properties.<sup>14</sup> A shear diagram for the switch blade is shown in Figure 3. Three forces  $P_1$ ,  $P_2$ , and  $P_3$  are acting on the switch blade at  $Z_1$ ,  $Z_2$ , and  $Z_3$ .

The deflection equation for the switch blade is calculated by the integral of the bending moment equation. The deflection of the switch blade is different in the AB, AC, and AD sections. The reaction force is calculated as  $R_a$ ,

$$R_a = -P_1 - P_2 - P_3 \quad (10)$$

The moment concerning the fixed point  $A$  is  $M_a$ ,

$$M_a = P_1 Z_1 + P_2 Z_2 + P_3 Z_3 \quad (11)$$

The bending moment  $M$  and the end deflection  $x$  are defined below:

Section A to B:

$$M = M_a + R_a Z \quad (12)$$

$$x = \frac{R_a Z^3}{6EI} \quad (13)$$

Section B to C:

$$M = M_a + R_a Z + P_1(Z - Z_1) \quad (14)$$

$$x = \frac{R_a Z^3 + P_1(Z - Z_1)^3}{6EI} \quad (15)$$

Section C to D:

$$M = M_a + R_a Z + P_1(Z - Z_1) + P_2(Z - Z_2) \quad (16)$$

$$x = \frac{R_a Z^3 + P_1(Z - Z_1)^3 + P_2(Z - Z_2)^3}{6EI} \quad (17)$$

The parameters used for the analytical bending equations (10), (11), (12), (13), (14), (15), (16) and (17) are derived from the switch rail presented in Table 1.

**Dynamic rail model.** The dynamic model adopts a finite element method. In the classical finite element method for analyzing the beam bending problem, the 2-node Hermite element is usually used.<sup>15</sup> Suppose the switch blade consists of 2 elements.

The stiffness and mass of each element is obtained as,

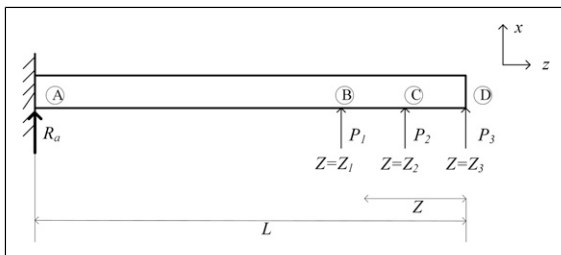


**Figure 3.** Schematic for horizontal deflection of the switch blade.

$$[k^e(t)] = \frac{EI}{Le^3} \begin{bmatrix} 12 & 6Le & -12 & 6Le \\ 6Le & 4Le^2 & -6Le & 2Le^2 \\ -12 & -6Le & 12 & -6Le \\ 6Le & 2Le^2 & -6Le & 4Le^2 \end{bmatrix} \quad (18)$$

$$[m^e(t)] = \frac{\rho A L e}{420} \begin{bmatrix} 156 & 22Le & 54 & -13Le \\ 22Le & 4Le^2 & 13Le & -3Le^2 \\ 54 & 13Le & 156 & -22Le \\ -13Le & -3Le^2 & -22Le & 4Le^2 \end{bmatrix} \quad (19)$$

where  $E$  is Young's modulus,  $I$  is the moment of inertia of the cross-section,  $A$  is the area of cross-section,  $Le$  is the length of a single element. Note that each switch blade is made up of many of these elements.

Due to the characteristics of the switch blade, the cross-sectional area and moment of inertia vary with the position. Starting from the front of the front toe, the cross-sectional area of the tip gradually widens. The cross-section is full until the distance at point  $Z$ , 5.037 m away from the front toe.<sup>13</sup> A 3D view of a switch blade model shows the change in cross-section, displayed in Figure 4.

The area  $A_i$  and moment  $I_i$  of inertia of the changed cross-section can be expressed by equations (20) and (21).  $L$  is the length of the rail and  $L_i$  represents the changeable length. The value range of the number  $i$  is from 1 to the mesh size.

$$I_i = \begin{cases} I \left[ 1 - \frac{L_i - Z}{16(L - Z)} \right] & (L > L_i > Z) \\ I(L_i \leq Z) \end{cases} \quad (20)$$

$$A_i = \begin{cases} A \left[ 1 - \frac{L_i - Z}{4(L - Z)} \right] & (L > L_i > Z) \\ A(L_i \leq Z) \end{cases} \quad (21)$$

The boundary condition corresponding to this switch blade model is to fix the point  $O$ , the element-wise stiffness and mass matrices are:

$$[K] = \frac{EI_i}{Le^3} \begin{bmatrix} 24 & 0 & -12 & 6Le \\ 0 & 8Le^2 & -6Le & 2Le^2 \\ -12 & -6Le & 12 & -6Le \\ 6Le & 2Le^2 & -6Le & 4Le^2 \end{bmatrix} \quad (22)$$

$$[M] = \frac{\rho A_i L e}{420} \begin{bmatrix} 312 & 0 & 54 & -13Le \\ 0 & 8Le^2 & 13Le & -3Le^2 \\ 54 & 13Le & 156 & -22Le \\ -13Le & -3Le^2 & -22Le & 4Le^2 \end{bmatrix} \quad (23)$$

The frictional force between the switch blades and the sleepers is included in this model. In this finite element model, the frictional force can be calculated as the product of the mass of one element and the frictional coefficient acting opposite to the motion of the switch blade. Combined with (21), the calculation formula of the friction force  $f_i$  of each element is:

$$f_i = \mu m g \frac{A_i}{A} \quad (24)$$

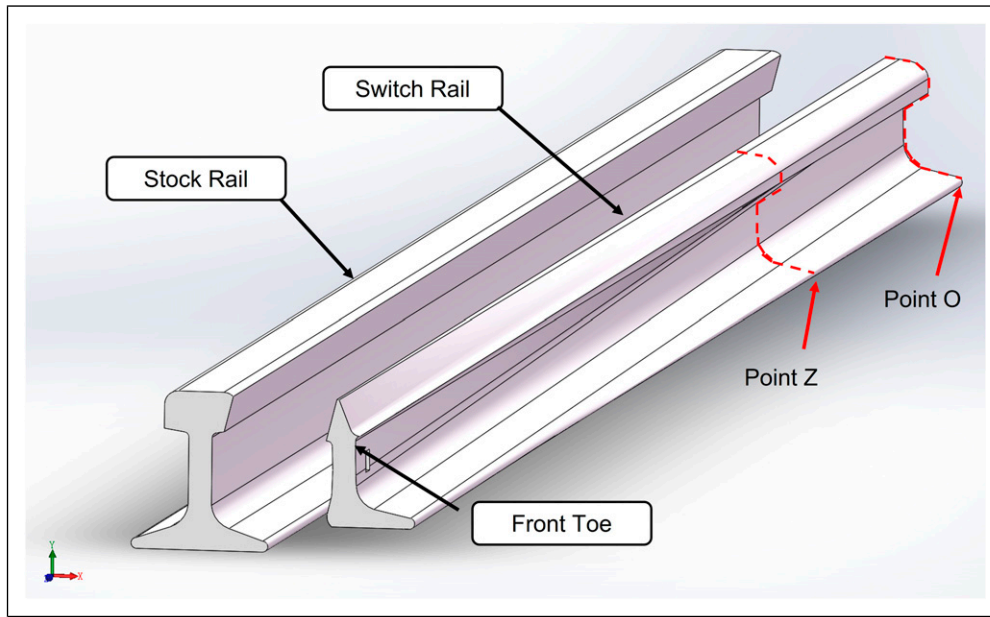


**Figure 4.** A 3D view of a switch blade model.

where  $m$  is the mass of one switch blade,  $g$  is the gravity acceleration,  $\mu$  is the coefficient of friction. The frictional coefficient can be adjusted according to actual requirements during application.

For dynamic simulation, the damping is considered as proportional Rayleigh damping<sup>16,17</sup> and the full dynamic system equations are written below.  $\vec{X}$  is the global displacement vector,  $\vec{F}$  is the global actuation force vector,  $\vec{f}$  is the full friction force vector. It is noticed that the actuation force has to overcome the full friction force distributing along the switch blade.

$$[M]\ddot{\vec{X}} + [C]\dot{\vec{X}} + [K]\vec{X} = \vec{F} - \vec{f} \quad (25)$$

$$[C] = c_0[M] + c_1[K] \quad (26)$$

where  $a_0$  and  $a_1$  are damping coefficient and stiffness coefficient. The values for  $a_0$  and  $a_1$  in this model are 1 and 0.6, respectively. These are derived from experimental results. One switch blade is now relatively modelled in equations (25) and (26).

Next, a pair of switch blades is built, and the schematic diagram is displayed in Figure 5. The switch rail  $A$  and the switch rail  $B$  are both composed of 20 elements. The red nodes are the joints. The illustration in the circle shows the principles of the two red nodes' connection.  $n_1$  and  $n'_1$  are the masses (matrices) of the nodes,  $u_1$  and  $u'_1$  are the forces,  $x_1$  and  $x'_1$  are the displacements.  $k$  and  $b$  correspond to the spring stiffness and damping coefficient, respectively.

According to Newton's second law, the force balance equation for  $u_1$  is:

$$u_1 - kx_1 - b\dot{x}_1 + kx'_1 + b\dot{x}'_1 = n_1\ddot{x}_1 \quad (27)$$

In the same way, the force equation for  $u'_1$  is:

$$kx_1 + b\dot{x}_1 - b\dot{x}'_1 + u'_1 = n'_1\ddot{x}'_1 \quad (28)$$

The values of  $k$  and  $b$  are 10,000 and 10,000,000, respectively, derived from experimental results.

A select function is made in Simulink to choose which red node or nodes should be rigidly connected. On this basis, each node acts as an excitation point to control its degree of freedom. External forces from the actuator can be applied at any node or nodes to observe the deformation state of the switch blades.

## Simulation results

A full track switch system simulation model is established in MATLAB/Simulink, including an actuator model and a switch blade model. Two parts of the results are discussed: switch blade bending analysis under full-scale parameters and simulation results when the electro-mechanical actuator is connected to the switch blades.

### Switch blade model results

Based on the previously discussed static bending analysis, the established finite element dynamics model can be verified. Note that there are three positions on the switch blade to bear the load of three points ( $P_1$ ,  $P_2$ , and  $P_3$ ), as presented previously in Figure 3. The three steps are:

- (i) discuss the results when applying an external force only at the position  $P_3$ ;
- (ii) compare the analytical results with the FE steady-state dynamic response in seven different situations;
- (iii) validate the forces against results obtained from Simpack.

**Single applied force.** A single point load increasing in steps of 100N from 0N to 1000N acts on the rail at  $P_3$  and the

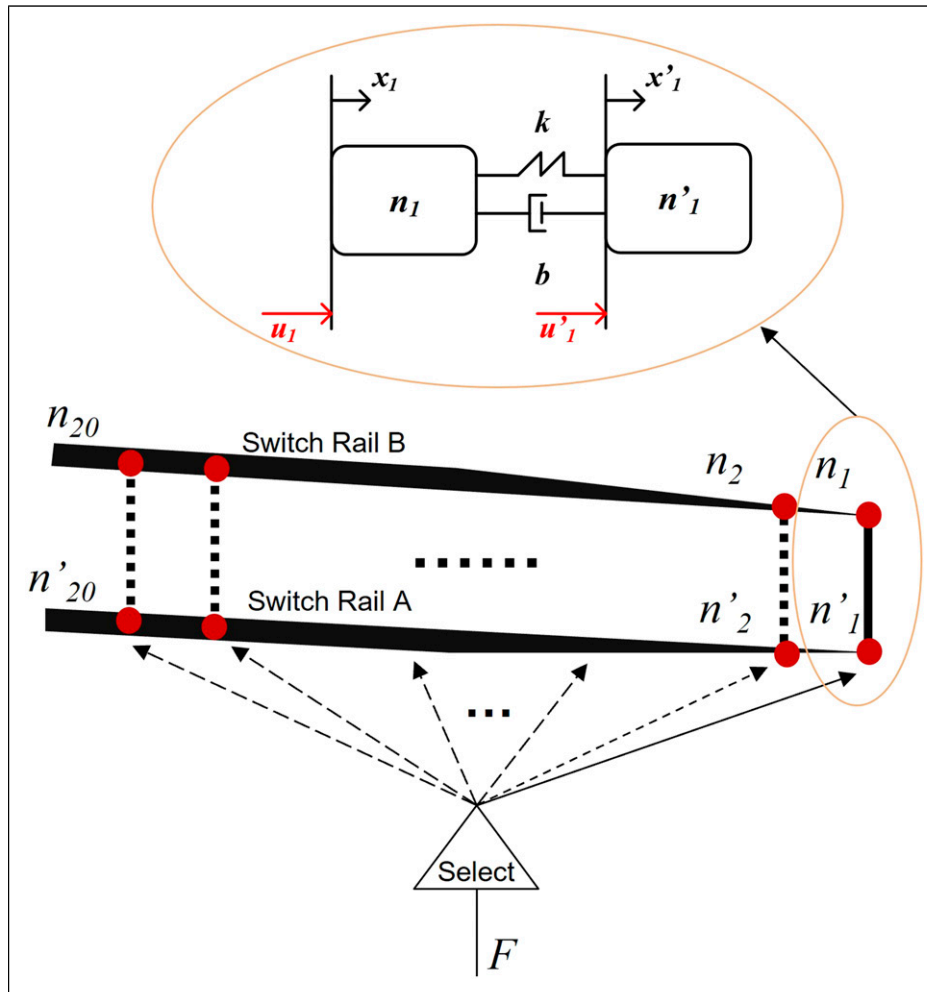


**Figure 5.** A schematic diagram of two switch blades.

other forces are set to 0. This test is used to identify rail deflections and evaluate the performance when different forces act on the front toe. The results obtained from the preliminary analysis shown in Figure 6(a) display the horizontal deflections of the rail. As the force increases, the deflection of the rail also increases, and the force that works on the end of the rail will cause the rail to deform in proportion to the applied force. The solid lines in the figure represent the analysed results, while the cross lines indicate the steady-state response of the dynamic results. It can be seen that the results obtained from these two analyses are in good agreement.

**Multiple applied forces.** Here different combinations of forces are applied along the length of the rail to observe the influence of multiple external forces on the switch blade. Three equal forces of 500N are applied to the three indicated positions  $P_1$ ,  $P_2$ , and  $P_3$ . Figure 6(b) illustrates the relationship between the deflection in each direction and the distance along the length of the rail. In this test, seven cases are discussed. The static analysed solution and the dynamic finite element simulation results are compared in each case. It can be seen that as the applied force increases, the deflection of the rail from left to right also increases. The solid lines in the figure represent the analysed results, while the

cross lines show the steady-state response of the dynamic results.

In the steady-state, there is a small difference between the static results and the dynamic deflection of each element along the track length, caused by the difference in the number of elements. The dynamic and static deflection is closest at the points where the individual forces  $P_1$ ,  $P_2$ , and  $P_3$  are applied along the length of the rail. The error of the deformations between the static model and the steady-state of the dynamic model is less than 4%.

**Validation against Simpack and experimental results.** Here, a constant force is considered as the input of the following validations. First, the input forces are validated against the experimental and Simpack forces, as listed in Table 2. It should be noted that the force here acts on the front toes of the two switch blades. The results in the third column are implemented in Simpack using the finite element method. As a one-off for model validation, Simpack is useful. However, when the Simpack and the control model (like MATLAB) are connected for co-simulation, it takes several hours to simulate each second. The comparison result shows that this paper's model performs very well for the switch blade.

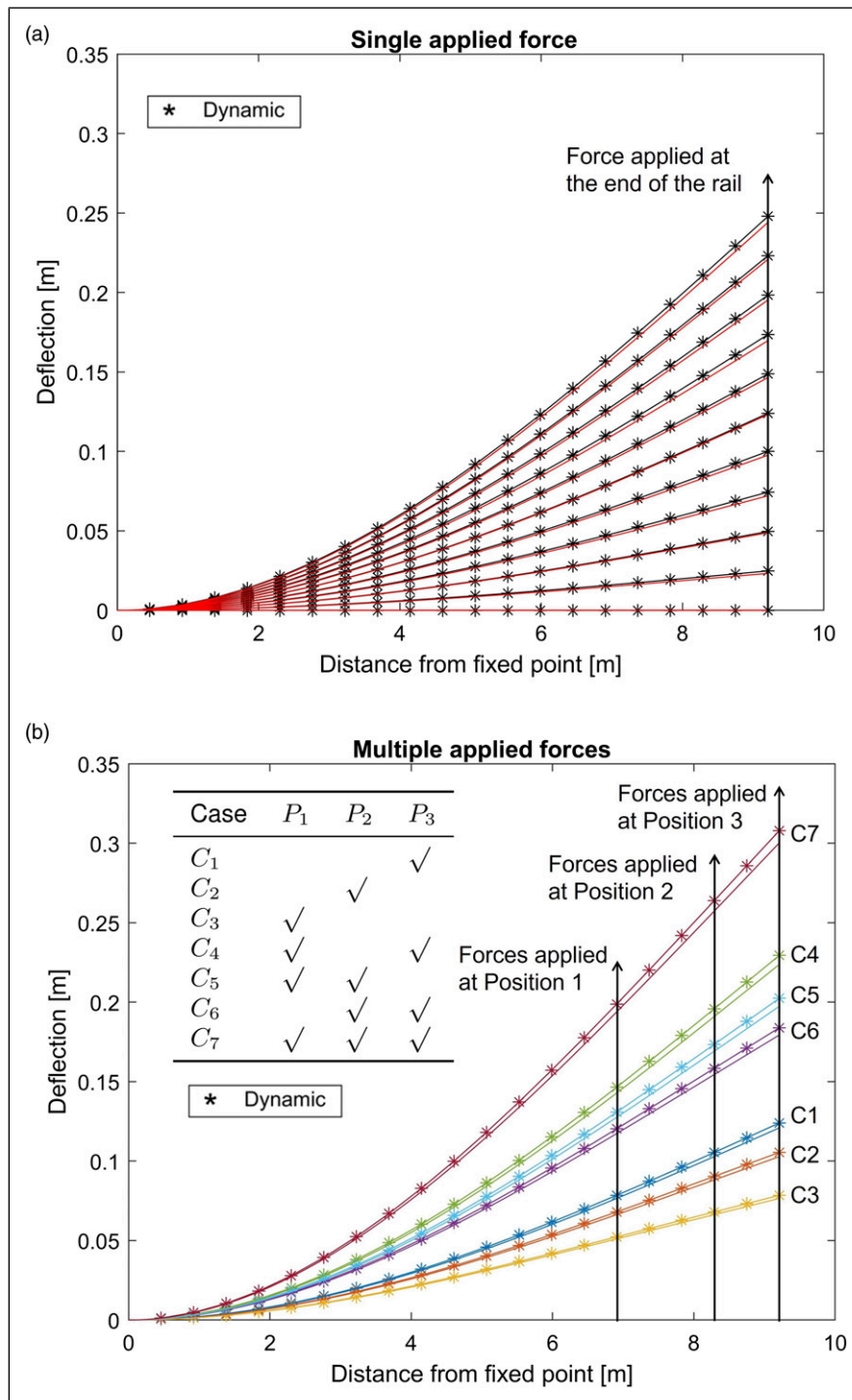


Figure 6. Rail bending when subjected to the different forces.

**Combined blade and actuator model results**

In this section, a complete switch model is compiled using MATLAB/Simulink, as shown previously in Figure 2. The input of the actuator model is voltage, and the output is the actuator force. The force is applied to the front toe position. This combined model is validated with the HPSS model built-in co-simulation of Simpack/

Simulink and the data details can be found in the reference [13]. The available data is the displacement of the front toe and the current of the DC motor, as displayed in Figure 7. The same command input step of a constant voltage of 120 V is applied to the Simulink model to cause a movement at time 1 s. Once the switch blade closes the gap at the corresponding stock rail, the motor current will rise and the motor will be switched off. The

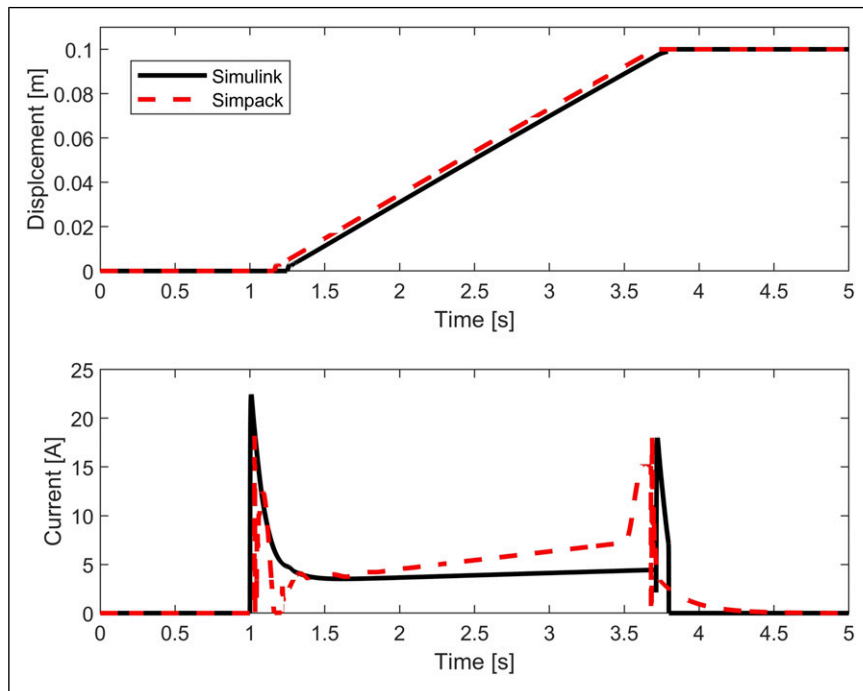
results show that at around 3.7 s, the front toe displacement can reach 0.1 m, which matches the required switch blade travel. The slight differences in the current

figure between the Simpack and Simulink models are due to the inclusion of some other mechanical connections in the original complicated Simpack model. Overall, the comparison between the simulation results and the available data shows that the model has a good fit. It can be concluded that the model is a good representation of the full switch system.

The paper's model requires 1.2 s of computational time to simulate 1 s, while the co-simulation costs several hours. Although the model built in Simulink is not as complex as Simpack, it has the great advantage of very fast computation time while still producing very similar results (error of the deformations <4%). That is to say, the switch model proposed in this paper can be used as a model for a series of other applications such as controller design, intelligent algorithm design, etc., thereby greatly improving the design efficiency. This is also the fundamental significance of this model. A summary comparison between the paper's model and the conventional co-simulation approach is presented in Table 3.

**Table 2.** Force comparisons of different methods.

y (mm)	Experimental Force (N)	Simpack Force (N)	Paper's dynamic Model force (N)
57.5	460	468	473.5
56.5	454	460	465.5
54	436	440	443.5
49.8	402	406	408.5
44	358	358	360.3
37	298	302	302.3
28.8	232	234	235
19.7	158	160	159.8
10	82	82	80.2
0	0	0	2



**Figure 7.** Model validation for the front toe displacement and the DC motor current.

**Table 3.** Comparison of paper's model and the co-simulation model.

	FE Simulink Track Switch Model	Co-simulation Track Switch Model
Differences	Build in Matlab/Simulink Significantly reduce the computational time Use easily and user friendly	Build in Co-simulation (Simpack and Simulink) 3D straightforward model More complex
Applications	Controller design, System validation or Other Matlab based design	Controller design, Railway surface analysis or Other Simulink based design
Computational Time (to simulate 1s) (apply with controller)	1.2 s 2 s	>3 h >4 h

## Conclusion

In this paper, a new approach to the dynamic modelling of railway track switches has been proposed. The model has been described and compared to static and dynamic results obtained using other methods. It has also been shown to be consistent (in terms of static forces and deflections) with experimental results. The outcome is that the model is judged to be valid in that it correctly predicts both the dynamic and static bending of the switch blades. It also has the benefit that it allows actuator forces to be applied along the length of the rails. These positions can be specified by the user/designer. Ultimately it was found that this model operates close to real-time and that it is an order of magnitude faster than similar models developed through co-simulation of MATLAB/Simulink with multi-body dynamics software such as Simpack.

It is intended that this model has a number of potential uses by researchers and engineers. Firstly, it can allow researchers to design, compare and evaluate safely a range of control system designs for railway track switches (which presently are all controlled open-loop). In addition, researchers can use the model to examine actuation options ranging from one actuator to several actuators distributed along the length of the switch. To facilitate these future uses by researchers, the complete model is made freely available and can be found here: <https://doi.org/10.25500/edata.bham.00000884> or can be obtained directly from the first author. In terms of future work, we note that it may be possible to model everything in Simpack (i.e. simulate the electro-mechanical actuator and control system in Simpack itself). This is something which could be investigated in the future.

## Declaration of conflicting interests

The author(s) declared no potential conflicts of interest with respect to the research, authorship, and/or publication of this article.

## Funding

The author(s) disclosed receipt of the following financial support for the research, authorship, and/or publication of this article: The work arising in this paper has received funding from the School of Engineering at the University of Birmingham. The author(s) are deeply grateful to the School of Engineering and Birmingham Centre for Railway Research and Education (BCRRE) for the resources provided.

## ORCID iDs

Linxiao Li  <https://orcid.org/0000-0003-1204-6586>  
Saikat Dutta  <https://orcid.org/0000-0002-9906-6477>

## References

- Bemment SD, Goodall RM, Dixon R et al. Improving the reliability and availability of railway track switching by analysing historical failure data and introducing functionally redundant subsystems. *Proc Inst Mech Eng F J Rail Rapid Transit* 2018; 232(5): 1407–1424.
- Lagos RF, Alonso A, Vinolas J, et al. Rail vehicle passing through a turnout: analysis of different turnout designs and wheel profiles. *Proc Inst Mech Eng F J Rail Rapid Transit* 2012; 226(6): 587–602.
- Cope GH. *British railway track: design, construction and maintenance*. Loughborough, UK. Permanent Way Institution Barnsley, 1993.
- Palli S, Koonra R, Sharma SK, et al. A review on dynamic analysis of rail vehicle coach. *Int J Veh Struct Syst (Ijvss)* 2018; 10(3).
- Andersson C and Dahlberg T. Wheel/rail impacts at a railway turnout crossing. *Proc Inst Mech Eng Part F J Rail Rapid Transit* 1998; 212(2): 123–134.
- Andersson C and Dahlberg T. Load impacts at railway turnout crossing. *Veh Syst Dyn* 1999; 33(sup1): 131–142.
- Bruni S, Anastasopoulos I, Alfi S, et al. Effects of train impacts on urban turnouts: modelling and validation through measurements. *J Sound Vibration* 2009; 324(3–5): 666–689.
- S-CODE. S-code. <https://www.s-code.info/>, 2020.
- In2rail. In2rail. <https://www.in2rail.eu/>, 2018.
- Wright N, Bemment S, Ward C, et al. A model of a repoint track switch for control. In: 2014 UKACC International Conference on Control (CONTROL), Loughborough, UK, 09–11 July 2014: IEEE, pp. 549–554.
- Sarmiento-Carnevali M, Harrison T, Dutta S, et al. Design, construction, deployment and testing of a full-scale repoint light track switch (i). In *The Stephenson Conference: Research for Railways, Institution of Mechanical Engineers (IMechE)*, London, UK, 25th–27th April 2017: Loughborough University, pp. 409–416.
- Olaby O, Dutta S, Harrison T, et al. Realisation of a novel functionally redundant actuation system for a railway track switch. *Appl Sci* 2021; 11(2): 702.
- Dutta S, Harrison T, Ward CP, et al. A new approach to railway track switch actuation: dynamic simulation and control of a self-adjusting switch. *Proc Inst Mech Eng Part F J Rail Rapid Transit* 2020; 234(7): 779–790.
- Paz M and Leigh W. *Integrated matrix analysis of structures: theory and computation*. New York. Springer Science & Business Media, 2012.
- Gunakala SR, Comissiong D, Jordan K, et al. A finite element solution of the beam equation via Matlab. *Int J Appl* 2012; 2(8): 80–88.
- Ling X and Haldar A. Element level system identification with unknown input with rayleigh damping. *J Eng Mech* 2004; 130(8): 877–885.
- Panzer H, Hubele J, Eid R, et al. *Generating a parametric finite element model of a 3d Cantilever Timoshenko Beam Using Matlab*. Technical report, München, Lehrstuhl für Regelungstechnik, 2009.